Growth Mechanism of Textured MgO Thin Films via SSCVD

Matthew R. Hill,† Everett Y. M. Lee,† Jennifer J. Russell,† Yu Wang,‡ and Robert N. Lamb*,†

Surface Science and Technology, School of Chemistry, and School of Materials Science, The University of New South Wales, Sydney, NSW 2052, Australia

Received: January 17, 2006; In Final Form: March 15, 2006

Magnesium oxide thin films have been deposited with use of single source chemical vapor deposition (SSCVD). The resultant films were examined by using transmission electron microscopy, X-ray texture analysis, and pole figure analysis. Due to the nature of the chemical reactions occurring at the surface during SSCVD growth, which result in a high growth rate/low flux environment, films of (111) orientation have been achieved without an amorphous underlayer, an unusual result for films of this orientation. Moreover the films have a strong degree of biaxial texturing in the $x-y$ plane as found with X-ray texture analysis. These findings have important implications for buffer layers in perovskite thin film devices. The mechanism producing these structures has been revealed by using TEM and is discussed here.

Introduction

MgO thin films have been grown via several methods including sol−gel,[1,2] e-beam evaporation,[3,4] MOCVD,[5] spray pyrolysis,[6−9] and pulsed laser deposition.[10,11] In each of these techniques several different preferred orientations have been observed depending on the growth parameters. Generally, at high precursor flow rates the films exhibit purely (111) orientation while at low flow rates (200) preferred orientation is obtained.

The growth of MgO films with a preferred (111) out-of-plane orientation seems unusual as this is not the most energetically favorable orientation. In the growth of fcc oxides the (200) orientation minimizes the surface free energy and is therefore more energetically favorable. However, the lower density (111) orientation has been shown to predominate as the fastest growing phase through an evolutionary process when the growth rate is sufficiently high.[12] The (200) orientation is formed when the growth rate is low enough to allow surface diffusion to occur, resulting in the formation of the most densely packed phase parallel to the substrate. When the growth rate is increased, generally by increasing the flow rate of matter to the substrate, the mechanisms of film growth become dominated by the incoming precursor adhering to one crystal plane in preference to another. This phenomenon results in an evolutionary process where the fastest growing plane dominates, eventually becoming the preferred orientation of the final film.[12]

As the growth of MgO thin films with a preferred (111) orientation is a competitive process it has been suggested that an amorphous layer is required to be deposited prior to preferred orientation developing.[9] This merely suggests that the initial film layer is of random orientation with preferential orientation developing as the deposition process continues. Renault and Labeau[9] found that the film was amorphous to a thickness of 150 nm after which the (111) orientation was seen to develop preferentially. This first 150 nm may be composed of very small grains which are smaller than the coherence length of the X-rays and hence unable to be detected by XRD.

One of the most common uses of MgO is as a buffer layer for the deposition of a variety of materials, particularly the perovskite oxides. Materials belonging to the perovskite family of ceramics have found applications in capacitors and, increasingly, in piezoelectric and ferroelectric devices.[10] The lattice dimensions of the perovskite oxide crystals such as $BaTiO_3$ or $LiNbO_3$ vary substantially from semiconductor substrates including Si and GaAs.[13] The lattice mismatch leads to problems of adhesion and orientation as well as causing the introduction of misfit dislocations at the interface thus degrading device performance. These problems can be overcome with the addition of a magnesium oxide buffer layer between the substrate and the perovskite film with the lattice mismatch between MgO and $BaTiO_3$ being just 4.2%.[14]

The crystallographic orientation of the MgO film is important when considering its effectiveness as a buffer layer. The orientation of MgO films depends largely on the growth technique and the conditions employed for the particular deposition. This is to be expected as the deposition technique will influence the nature of reactions occurring at the growing surface by altering factors including growth rate and precursor flux.

In the present study films were deposited via SSCVD. The resulting films were solely of (111) out-of-plane orientation and, unlike films grown in previous studies, are free of an amorphous underlayer. A novel growth mechanism that accounts for the results obtained from Transmission Electron Microscopy and X-ray texture mapping is described. It is based on an understanding of the interfacial chemistry and decomposition processes.

Experimental Section

Films were deposited via SSCVD on Si(100) substrates that were ultrasonically cleaned in organic solvents. No attempt was made to remove the native oxide layer from the substrates. $Mg_6(O_2CNEt_2)_{12}$ (**1**) was used as the single molecular precursor for all depositions. No carrier gases were required to transport the volatilized precursor to the substrate. The synthesis of compound **1** has been described previously.[15−17] Against a background pressure of 3×10^{-7} Torr, the precursor was

* Address correspondence to this author. E-mail: r.lamb@unsw.edu.au.
† Surface Science and Technology, School of Chemistry.
‡ School of Materials Science.

10.1021/jp060335o CCC: $33.50
Published on Web 04/14/2006

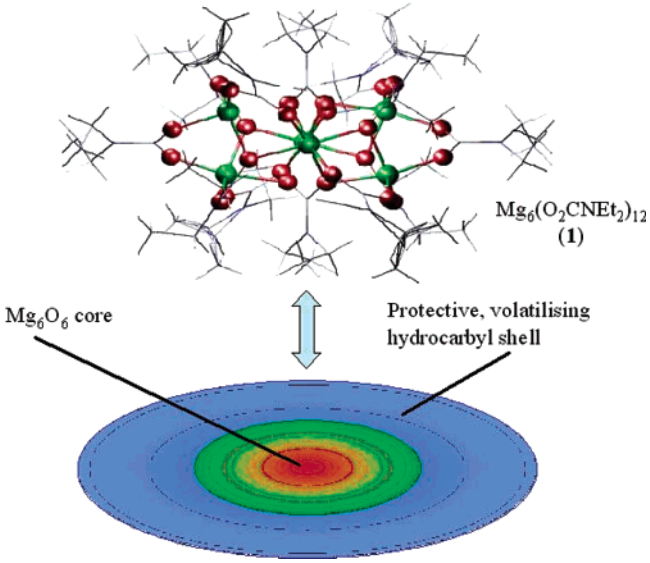

Figure 1. Molecular structure of MgO precursor.

evaporated at a precursor partial pressure of 5×10^{-6} Torr. Deposition was performed at the optimal substrate temperature of 550 °C.[15] The silicon wafer was positioned normal to the direction of precursor flux and 5 cm from the Knüdsen cell aperture. The deposition rate was relatively high (~1 μm/h) even when the precursor flux was kept low. The growth time was varied from 10 min to 2 h in order to obtain films with thicknesses ranging from 100 nm to 2 μm. Transmission electron microscopy was performed with a Philips CM200 FEG TEM operating at an accelerating voltage of 200 kV. Films were thinned by using an FEI ×P200 focused ion beam miller. Samples were coated with a 1 μm thick Pt layer to prevent charging prior to examination in TEM. XRD was carried out with a Philips X'pert MRD system, using a Cu tube (wavelength 1.5418 Å) and the conditions of 30 kV and 50 mA. A capillary lens was used in the primary beam side. $\theta-2\theta$ scans were conducted to determine the orientation and a φ scan, with tilted ψ, to measure the textures.

Results and Discussion

The SSCVD technique differs from conventional CVD and indeed from most other chemical deposition techniques because all film constituents are supplied from one molecule and no carrier gases are used during the deposition. The exact setup of the technique has been described previously.[18] The precursor molecule consists of a core containing the constituent film components surrounded by organic ligands arranged to impart volatility to the molecule. A precursor molecule is sublimed from a heated evaporation cell onto a hot substrate at which the organic ligands thermally decompose into volatile byproducts, with the metal oxide residue remaining on the substrate to form a crystalline thin film. An effective precursor decomposes cleanly so that the byproducts are not incorporated into the film. The optimum parameters for such a precursor have been determined previously.[15] The use of a single precursor molecule greatly simplifies the deposition process, and changes the nature of reactions occurring at the growth interface.

The precursor used for the growth of these films is $Mg_6(O_2CNEt_2)_{12}$ (**1**) and can be regarded as structurally consisting of a volatility inducing, protective hydrocarbyl outer shell that surrounds an ordered core of MgO, as shown in Figure 1. When the outer shell detaches at the hot substrate, the pre-ordered Mg_6O_6 metal oxide core remains, which then readily coalesces

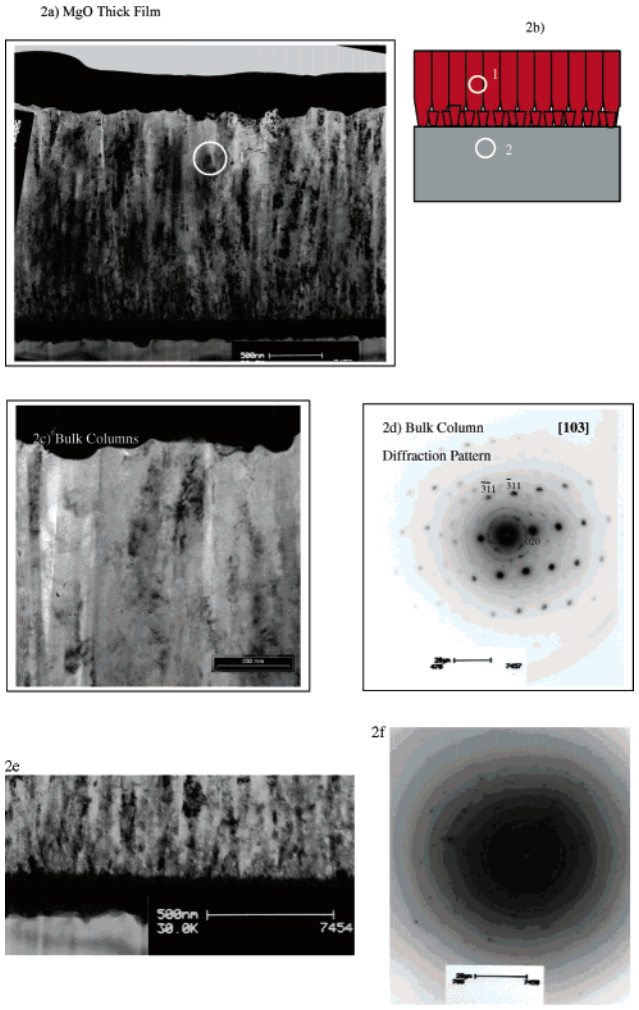

Figure 2. (a) Cross-sectional TEM image of the MgO thick film. (b) Schematic showing the film growth mechanism. (c) Cross-sectional TEM image of the bulk region of the film. (d) Electron diffraction pattern from a single bulk column confirming orientation. (e) The cross-sectional TEM image of the interface shows a large number of thin columns. (f) Electron diffraction pattern from the interfacial region. A dotted ring pattern as the beam size is greater than the width of one column.

onto the substrate to form a crystalline thin film. Previously, it was shown that this precursor could be used for SSCVD to deliver MgO thin films of purely (111) orientation, with the lowest levels of carbon yet reported in the field.[15]

MgO films of varying thickness were deposited in order to investigate the evolution of structure in the SSCVD growth of this material. When depositing films to act as a buffer layer, they must be much thinner than those usually deposited with this technique. The purpose of the present work is to investigate the properties of ultrathin films deposited which have not previously been deposited by SSCVD and determine the structural suitability of these films as buffer layers.

Transmission Electron Microscopy (TEM) provides direct evidence of detailed cross-sectional morphology of the films.

Thick MgO films (~2 μm) were first examined to provide a comparison with the thin films. The thick MgO films exhibit purely (111) orientation perpendicular to the substrate.[15] The thick MgO films consist of well-defined columns as shown in the TEM image in Figure 2a. The images show that these films consist of two distinct regions: the bulk, where steady-state growth occurs, and the interfacial region, where the columns begin to coalesce and expand rapidly. The region labeled as

the interfacial region extends for the first 500 nm of film growth. After this point the familiar v-shaped growth is seen.[19] This is indicative of a competitive columnar growth process that has rarely been observed in SSCVD films but has been well characterized in evaporative growth methods.[19] Figure 2b shows a schematic of this situation in which the interface region consists of a large number of small columns with fewer, larger columns seen in the bulk region of the film.

The bulk growth region of the film is shown in greater detail in Figure 2c. The columns in this region are ~200 nm in diameter and appear highly crystalline. The dark/uneven regions in the image were attributed to surface damage that occurred during ion beam thinning. TEM can also be used to investigate the crystallographic orientation of the films. Using TEM it is possible to determine the local orientation as opposed to XRD, which shows the average orientation. The electron diffraction pattern of a single bulk column is shown in Figure 2d with the incident electron beam aligned on the [103] zone axis. The major reflections were identified, and confirmed the cubic structure of MgO. This indicates that the large columns in the bulk of the film are single crystals of MgO that are essentially free of crystallographic defects. The electron diffraction pattern remained constant when the beam was moved along the length of the bulk columns but changed when moved onto adjacent columns. This indicates that the film was polycrystalline with a (111) out-of-plane orientation but that the in-plane orientation is not constant across the film.

The crystallographic structure of the interfacial region is of most importance since this is most likely to resemble an ultrathin film. This region consists of a large number of thin columns and the diffraction pattern appears as a dotted ring pattern as shown in Figure 2e,f. As the spot size of the electron beam (250 nm diameter) is much larger than the width of the individual columns in this region (~30−50 nm diameter) it was not possible to obtain a diffraction pattern from an individual column. The dotted ring pattern is consistent with the averaging of several crystalline columns. There is no evidence of the expected amorphous underlayer from the TEM images or diffraction patterns. The images show that the columns originate directly from the substrate.

While the out-of-plane orientation is important for buffer layer growth, the in-plane orientation is perhaps even more crucial. To act as an effective buffer layer the film must possess some degree of biaxial texturing and be as close to single crystal as possible. Neither electron diffraction nor conventional XRD can provide details of the degree of in-plane coherence. For this purpose X-ray pole figure analysis was performed. If the film is randomly oriented on the substrate a ring pattern would be observed in the pole figure analysis. If the (111) MgO film is epitaxially deposited on the Si(100) substrate, three points would be seen at 120° intervals. Figure 3 shows the pole figure of a thick MgO film along the (111) axis. Several discrete points can be seen on the pole figure, meaning that the film is not randomly oriented on the substrate. In this analysis eight discrete points are seen. It appears that the individual columns exist in one of only three orientations on the substrate. It follows then that the ordered substrate is directly influencing the in-plane orientation of the film. This is direct evidence of the absence of an amorphous layer close to the substrate since such a layer would prevent the substrate from affecting in-plane coherence.

A cross-sectional TEM image from a thin MgO film is shown in Figure 4a. The film is ~200 nm thick and consists of small columns which grow from the substrate to the surface of the film. These columns are identical with those observed in the

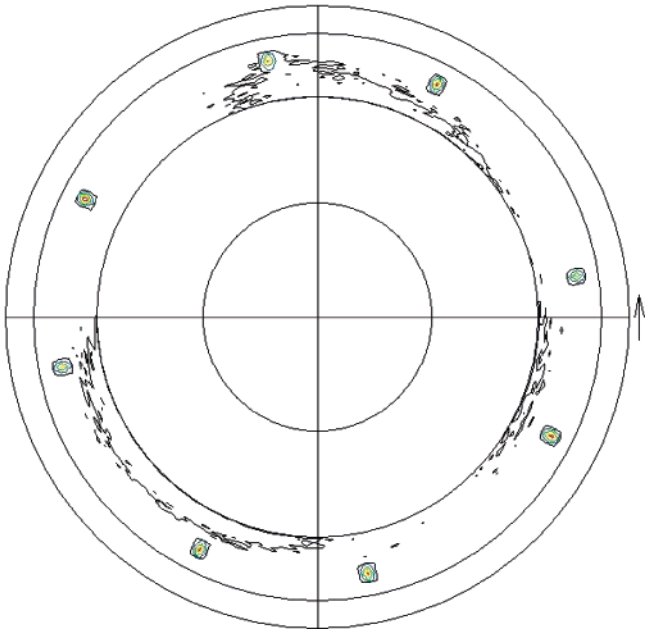

Figure 3. Pole figure analysis of the MgO thick film showing several discrete points indicating nonrandom in-plane orientation.

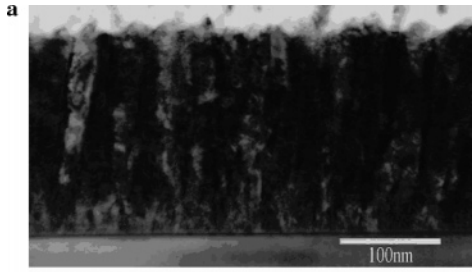

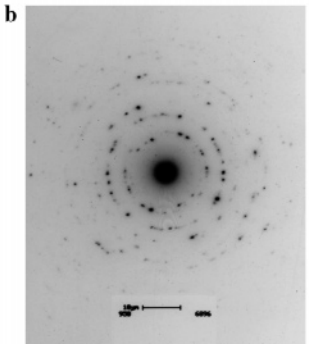

Figure 4. (a) Cross-sectional TEM image of the MgO thin film. (b) Electron diffraction pattern from a thin MgO film showing similar properties to the interfacial region of the thick MgO film.

interfacial region of the thick film as seen in Figure 2e. It is apparent that the film growth ceased in this sample prior to the formation of the large columns seen in the bulk region of the thick film. The electron diffraction pattern taken from this film is shown in Figure 4b. The pattern is similar to that of the interfacial region of the thick film with a polycrystalline ring pattern obtained. Again, this was due to the beam size being larger than the width of a single column. These results show that the properties of the interfacial region of the thick films are comparable with those of the thin films.

XRD texture analysis was performed to measure the change in the degree of crystallinity in films as a function of thickness. Figure 5 shows the texture analysis of the thick MgO film. It shows a strong (111) orientation but with some deviation of the columns from the normal to the surface. The texture analysis

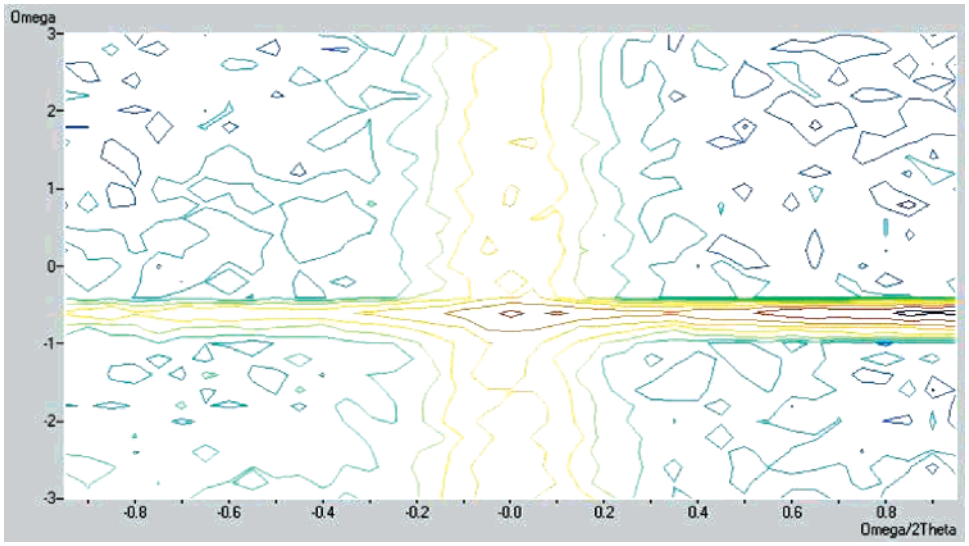

Figure 5. X-ray texture analysis from the MgO thick film showing a strong (111) orientation.

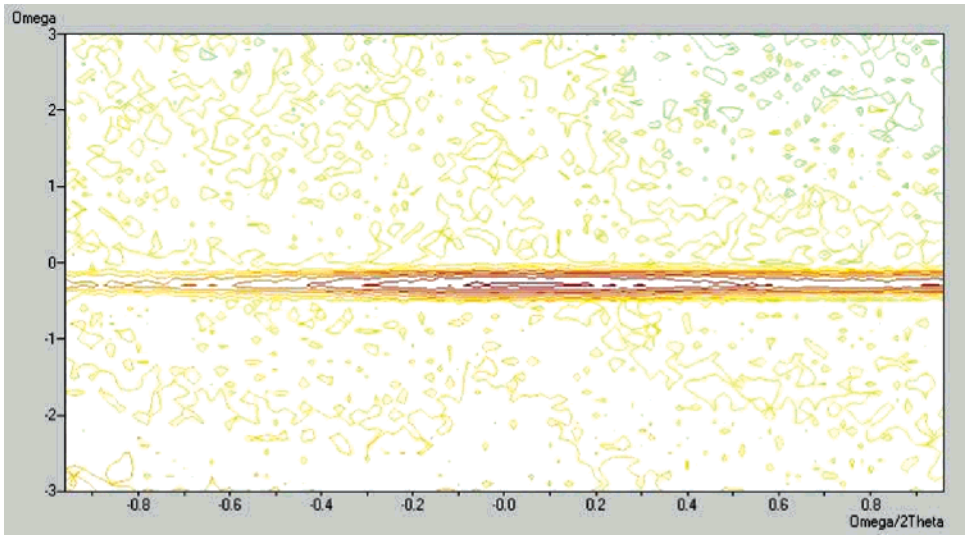

Figure 6. X-ray texture analysis from the MgO thin film showing a more uniform (111) orientation than that of the thick MgO films.

from the thin MgO sample is given in Figure 6. In this case the alignment of the (111) columns is much more uniform as indicated by the single set of contours centered at 0° $\omega/2\theta$. This finding contradicts the previous studies which suggest that the growth of the (111) orientation is evolutionary and requires an amorphous underlayer. If this were the case it would be expected that the thinner films would be less oriented than the thick films. The results of the texture analysis are in good agreement with the TEM images from both films which show the development of coherent columns directly from the substrate. The high degree of uniformity in columnar directionality for thin films as evidenced by XRD texture analysis bodes well in the use of these films as buffer layers.

Since all the film constituents for SSCVD are contained within one molecule, there is no secondary reaction that needs to occur at the substrate before a film can be formed. Other deposition techniques require oxidation of a metal-rich residue to form a stoichiometric mix or removal of carbonaceous contaminants via reaction or annealing. In the case of SSCVD growth the film coalesces directly from the precursor, and the rate limiting steps are eliminated so films grow at a faster rate. This rapid growth occurs even when the precursor flux is relatively low (see experimental details). Moreover, each precursor molecule delivers 6 MgO units to the substrate, so the rate of flow of volatilized precursor is comparably low in the context of how many units of MgO are delivered to the growth interface from each precursor molecule. Therefore, films are grown in a high growth rate, low flux environment. The formation of the highly crystalline thin films and the degree of in-plane coherency seen can be explained in terms of the chemical processes occurring during deposition, as shown in Figure 7. As mentioned previously, the fastest growing orientation will dominate the film by an evolutionary process once a sufficient thickness is reached. Figure 7 demonstrates that with the large MgO precursor core used in this study, this thickness is reached in very few interfacial reactions. As a result there is no initial growth of other phases unlike with precursors possessing smaller MgO cores.

Figure 8 shows an XRD of a film grown at high flux (ca. 2×10^{-5} Torr precursor partial pressure). When there is a greater amount of precursor impingent upon the growth interface all possible orientations grow at a high rate, with the crystallites reaching sufficient size to be identified by XRD before columns of the fastest growing phase crowd out other orientations. Under these conditions the low flux growth mechanism is superseded by the rapid precursor influx onto all crystal faces. This experimental evidence gives weight to proposed conditions and mechanisms under which the other films described are formed.

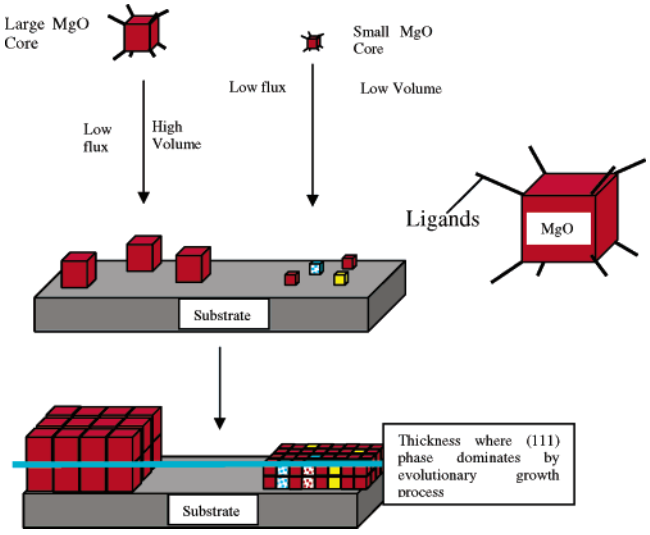

Figure 7. Schematic representation of the proposed growth mechanism.

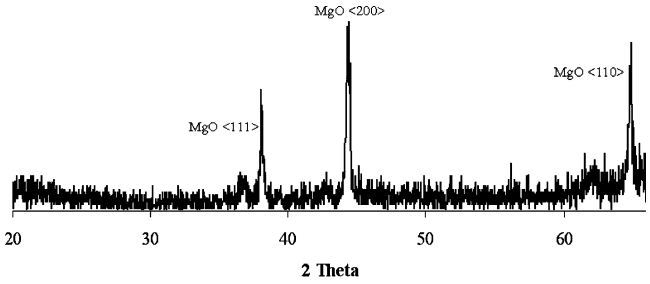

Figure 8. X-ray diffraction pattern of the MgO film grown under high flux conditions.

The unusual conditions of low flux and high growth rate witnessed in films grown through the SSCVD of the carbamate **1** provide a good basis for understanding the mechanism of (111) oriented film growth without an initial amorphous phase for self-texturing. A high growth rate means that the crystal face with the highest sticking probability will crowd out any other phases, and deliver a film in which the (111) plane dominates. A low flux, on the other hand, implies that a negligible amount of matter will have impinged on the substrate before the preferred growth of the (111) plane sufficiently dominates over the favored (200) growth direction.

The growth phenomena outlined in this paper have important implications for the development of ultrathin MgO films for device applications where a single preferred orientation is necessary in the use of buffer layers or as heterogeneous catalysts. As insufficient buffer layer texturing can adversely affect the quality of devices it is important to achieve the preferred (111) orientation in thin films without an amorphous underlayer. It has been shown that such films can be grown simply and efficiently by using single source chemical vapor deposition.

Conclusion

High-quality MgO thin films of purely (111) orientation have been deposited by using SSCVD without the initial formation of an amorphous underlayer. TEM images show that films of ~100 nm thickness exhibit well-defined columnar growth. XRD texture analysis indicated that the crystallites within these columns are more distinctly aligned than when film thickness is increased, indicating that thinner films are indeed more suitable for use in multilayer devices of complex oxide thin films. X-ray pole figure analysis shows that the thick film is in-plane coherent due to influence from the ordered substrate, providing direct evidence for the absence of an amorphous underlayer. The unusual growth conditions at the deposition interface were highlighted, and it was proposed that a combination of a high growth rate occurring despite a low precursor flow to the substrate accounted for the growth of the less energetically favored form of MgO, without a significant growth competition process being necessary to facilitate its formation.

These results show that precursor **1** provides a means of growing a (111) MgO film in a quick and simple manner that is suitable for device applications even when deposited in very thin layers.

Acknowledgment. The authors thank the Australian Postgraduate Award Scheme for financial assistance.

References and Notes

(1) Yoon, J.-G.; Kim, K. *Appl. Phys. Lett.* **1996**, *68*, 2523.

(2) Yoon, J.-G.; Kim, K. *Appl. Phys. Lett.* **1995**, *66*, 2661.

(3) Huhne, R.; Fahler, S.; Holzapfel, B.; Oertel, C.-G.; Schultz, L.; Skrotzki, W. *Physica* **2002**, *372*−*376* 825.

(4) Weber, T. P.; Ma, B.; Balachandran, U.; McNallan, M. *Thin Solid Films* **2005**, *476*, 79.

(5) Sung, M. M.; Kim, C.; Kim, C. G.; Kim, Y. *J. Cryst. Growth* **2000**, *210*, 651.

(6) Stryckmans, O.; Segato, T.; Duvigneaud, P. H. *Thin Solid Films* **1996**, *283*, 17.

(7) Yoon, J.-G.; Hyun, K.-O.; Lee, S.-J. *Phys. Rev. B: Condens. Matter Mater. Phys.* **1999**, *60*, 2839.

(8) Kim, S. G.; Kim, J. Y.; Kim, H. J. *Thin Solid Films* **2000**, *376*, 110.

(9) Renault, O.; Labeau, M. *J. Electrochem. Soc.* **1999**, *146*, 3731.

(10) Masuda, A.; Yamanaka, Y.; Tazoe, M.; Nakamura, T.; Morimoto, A.; Shimizu, T. *J. Cryst. Growth* **1996**, *158*, 84.

(11) Chen, T.; Li, X. M.; Zhang, S.; Zeng, H. R. *J Cryst. Growth* **2004**, *270*, 553.

(12) Dong, L.; Srolovitz, D. J. *J. Appl. Phys.* **1998**, *84*, 5261.

(13) Zeng, J. M.; Wang, H.; Shang, S. X.; Wang, Z.; Wang, M. *J. Cryst. Growth* **1996**, *169*, 474.

(14) Yu, Y. *Ferroelectric Materials and their Applications*; North-Holland Press: Amsterdam, The Netherlands, 1991.

(15) Hill, M. R.; Jones, A. W.; Russell, J. J.; Roberts, N. K.; Lamb, R. N. *J. Mater. Chem.* **2004**, *14*, 3198.

(16) Yang, K.-C.; Chang, C.-C.; Yeh, C.-S.; Lee, G.-H.; Peng, S.-M. *Organometallics* **2001**, *20*, 126.

(17) Caudle, M. T.; Nieman, R. A.; Young, V. G., Jr. *Inorg. Chem.* **2001**, *40*, 1571.

(18) Tran, N. H.; Hartmann, A. J.; Lamb, R. N. *J. Phys. Chem. B* **2000**, *104*, 1150.

(19) Messier, R.; Venugopal, V. C.; Sunal, P. D. *J. Vac. Sci. Technol. A* **2000**, *18*, 1538.